Applied Geochemistry 152 (2023) 105643

Contents lists available at ScienceDirect

Applied Geochemistry

journal homepage: www.elsevier.com/locate/apgeochem

# Implications of the Riverine Response to Enhanced Weathering for $CO_2$ removal in the UK

K.J. Harrington *, R.G. Hilton, G.M. Henderson

*Department of Earth Sciences, University of Oxford, 3 South Parks Road, OX13AN, UK*

ARTICLE INFO

Editorial Handling by: G. Bird

*Keywords:*
Enhanced silicate weathering
Carbon dioxide removal
Negative emissions
Carbonate precipitation
Geoengineering

ABSTRACT

Enhanced silicate weathering, the application of crushed calcium and magnesium-rich rocks to arable cropland, has been proposed as a potential negative emissions technology for the drawdown of atmospheric $CO_2$. Previous estimates have suggested that enhanced silicate weathering (EW) has the potential to remove significant quantities of $CO_2$, as much as 6–30 Mt $CO_2$ $yr^{-1}$ for the UK. However, if secondary carbonates are precipitated during the riverine transport of the products of EW, a portion of this $CO_2$ will be re-released, lowering the net carbon dioxide removal (CDR) potential of the mitigation strategy. Here, we assess the fluvial response to EW in the UK by calculating the expected riverine carbonate precipitation due to the dissolution of 10–50 t $ha^{-1}$ $yr^{-1}$ of silicate rock on available arable cropland in major UK catchments.

Increases in calcite saturation due to the export of soluble cations sourced from EW from soil to rivers are simulated to cross thresholds for spontaneous carbonate precipitation in several major UK river catchments (e.g. the Great Ouse, Thames). Catchments most susceptible to potential secondary carbonate precipitation are those with a high ratio of cropland to water discharge. On average, carbonate precipitation for major UK catchments is expected to make EW 16% (10 t $ha^{-1}$), 21% (20 t $ha^{-1}$) or 27% (50 t $ha^{-1}$) less effective at removing $CO_2$ than that predicted in the absence of such precipitation. Furthermore, when placing strict silica limitations on weathering reactions within soils, the CDR potential of EW is reduced considerably, to 0.23 Mt $CO_2$ $yr^{-1}$.

Although reducing the CDR potential of EW, we suggest that under rapid weathering conditions, carbonate precipitation in UK rivers will prevent pH increases over the safe level for freshwater ecosystems (pH > 9). Together, the simulations suggest that ambient hydrological conditions may make certain UK agricultural areas less effective for CDR by EW and call for methods to quantify secondary carbonate precipitation in response to EW treatments and to further investigate the role of silica saturation in suppressing weathering reactions.

## 1. Introduction

Humanity will need to employ various strategies over the coming century to halt increasing global temperatures and prevent catastrophic impacts of climate change (IPCC, 2018). One strategy will be to sequester $CO_2$ from the atmosphere using several proposed negative emissions technologies developed over the last two decades (The Royal Society and Royal Academy of Engineering, 2018). Enhanced silicate weathering (EW) has been suggested as a valuable method for atmospheric carbon dioxide removal (CDR) and relies on applying crushed calcium- and magnesium-rich silicate rocks to arable cropland (Hartmann et al., 2013; Beerling et al., 2018, 2020).

Enhanced weathering aims to speed up the natural process of rock dissolution, normally of silicates. An example is the dissolution of forsterite (Eq. (1)) which removes up to 2 mol of carbon dioxide from the atmosphere for every 1 mol of $Mg^{2+}$ released from the mineral:

$$Forsterite: Mg_2SiO_4 + 4CO_2 + 4H_2O \rightarrow 2Mg^{2+} + 4HCO_3^- + H_4SiO_{4(aq)} \quad (1)$$

Estimates suggest that globally upscaling EW, by applying between 10 and 30 tonnes of silicate rock (e.g., basalt) per hectare onto 900 Mha of equatorial cropland, has the potential to sequester 1.8–14.7 Gt $CO_2$ cumulatively by 2100. Early assessments of EW for the UK, e.g. (Renforth, 2012; The Royal Society and Royal Academy of Engineering, 2018), involving spreading between 10 and 20 t $ha^{-1}$ of silicate over half of the country's agricultural land suggested sequestration of 12–21 $MtCO_2$ per year (2.4–4.2% of the UK's annual emissions). A recent more sophisticated model of EW for the UK suggests sequestration potential of 6–30 $MtCO_2$ per year by 2050 from repeated additions to agricultural

* Corresponding author.
*E-mail address:* kirsty.harrington@st-annes.ox.ac.uk (K.J. Harrington).

https://doi.org/10.1016/j.apgeochem.2023.105643
Received 26 October 2022; Received in revised form 17 March 2023; Accepted 22 March 2023
Available online 24 March 2023

soils (Kantzas et al., 2022). These estimates suggest the potential for EW to contribute to the UK's legally binding 2050 net zero emissions target.

The CDR potential of EW is, however, reduced by at least six processes that have been recognized by a number of previous studies (Köhler et al., 2010; Fuhr et al., 2021; Klemme et al., 2022; Knapp and Tipper, 2022).

i. Precipitation of secondary carbonates in the soil (i.e. pedogenic carbonates)
ii. Silica saturation of soil waters limiting dissolution rates according to rainfall water supply
iii. Precipitation of secondary silicates (e.g. clays) in the soil, which alleviates silica saturation, but also removes some cations released from the primary silicate dissolution.
iv. Precipitation of secondary carbonates in rivers as products are carried from soil to ocean.
v. Estuarine mixing, during which the high alkalinity of seawater decreases the ratio of carbon for a given increase in alkalinity.
vi. Biotic (or inorganic) carbonate precipitation in seawater.

In this riverine study, we focus on an aspect that has not been well quantified: assessing the potential for reduced effectiveness of EW due to carbonate precipitation in rivers (point iv). We also consider the role of silica saturation and clay mineral precipitation (points ii and iii), given the importance of riverine discharge in transporting products, including Si, away from the soil.

When a mole of divalent cation ($Ca^{2+}$ and $Mg^{2+}$) is released from primary minerals into freshwater with a close to neutral pH, the excess positive charge is mostly balanced by $HCO_3^-$ (e.g., equation (1)) resulting in the uptake of 2 mol of atmospheric $CO_2$ into the water. However, if mineral saturation levels in the water result in the precipitation of secondary carbonate, 1 mol of this $CO_2$ is re-released to the atmosphere (Equation (2)), lowering the net drawdown efficiency of EW:

$$\begin{matrix} Secondary\ Carbonate\ Precipitation: \\ Ca^{2+} + 2HCO_3^- \rightarrow CaCO_3 + CO_2 + H_2O \end{matrix} \quad (2)$$

Secondary carbonate minerals can form in soil, during riverine transport, or in the oceans. Previous studies have reported the link between secondary carbonates and the reduced drawdown efficiency of EW (Renforth, 2019; Kantzas et al., 2022), and it has gained recognition as an important variable, which two recent studies highlight. Kantzas et al. (2022) reduced the overall CDR potential by 10–15% to account for ocean outgassing and (oceanic) carbonate precipitation in their model-based CDR calculations for EW in the UK. They also suggest that the alkalinity generated by EW increases the quantity of $CaCO_3$ precipitation in soils over time. Knapp and Tipper (2022) consider the global impact of carbonate precipitation during riverine transport of the products of enhanced carbonate weathering (e.g. via liming of agricultural land). Their study suggests that the dissolved products may be transported to the ocean if global rivers can maintain disequilibrium with respect to calcite (upholding a calcite saturation index of 1), however two thirds of the sequestered $CO_2$ via any enhanced carbonate weathering will be re-released due to secondary carbonate precipitation under equilibrium conditions (precipitation occurring at a saturation index = 0).

Additionally, to determine whether riverine transport of the products of EW would be a limiting factor, a conceptual model-based study by (Zhang et al., 2022) took baseline carbonate chemistry from US and global rivers and iteratively added ions from stoichiometric rock weathering until the water reached a specified saturation required for carbonate precipitation (as the exact value for this is unknown, they testedvarious calcite saturation states (Ω), between Ω = 5–25). They found that over baseline levels, global rivers could transport an extra 7–21.3 Gt $CO_2$ $yr^{-1}$ of EW derived $CO_2$ before significant carbonate precipitation would lower the overall efficiency of EW.

Here, we build on their contributions by taking a catchment specific approach to question what the traditional spreading scenarios (10–50 t $ha^{-1}$ $yr^{-1}$) will do to the carbonate chemistry of individual UK catchments. We suggest that because of the uneven distribution of UK arable land, there is a potential for large variations in the flux of EW derived ions to rivers. This heterogeneity may mean that, for catchments with low arable land, the potential $CO_2$ transport capacity as suggested by (Zhang et al., 2022) will not be met, whilst catchments with high arable land may cross thresholds for precipitation and cause reductions in the overall CDR efficiency of EW.

The flux of ions to the river will be controlled by the complexities of the soil environment. Environmental conditions in the soil-such as temperature (Pogge von Strandmann et al., 2022), pH, availability of water (Buckingham et al., 2022), and the extent of biological activity (Vicca et al., 2022), will determine the weathering rates of the applied silicate and dissolution may be suppressed when conditions for weathering are not ideal (Brantley et al., 2023). Once the applied silicate dissolves, soil processes, such as secondary mineral formation (secondary clays and pedogenic carbonates), cation exchange on soil mineral surfaces, equilibrium reactions in soil porewaters (Köhler et al., 2010), and plant uptake of cations (Kelland et al., 2020) may reduce the quantity of ions to leave the soil and enter the river. In contrast to the riverine environment, the impact of soil processes on the kinetics of weathering has been the subject of many studies, and therefore it is not the focus here. However, we do consider once area of the soil environment which may significantly influence the flux of ions to rivers: the release of silicic acid during dissolution.

The release of silicic acid during weathering reactions may limit the CDR achievable by EW. During weathering, silicate minerals may dissolve completely, releasing cations and silicic acid into surrounding waters (e.g. Equation (1)). Alternatively, they may preferentially release base cations into solution whilst retaining silica and some cations in secondary minerals, for example, the alteration of anorthite to kaolinite (equation (3)):

$$\begin{matrix} Anorthite\ dissolution: \\ CaAl_2Si_2O_8 + 2CO_2 + 3H_2O \rightarrow \\ Ca^{2+} + 2HCO_3^- + Al_2Si_2O_5(OH)_4 \end{matrix} \quad (3)$$

When weathering reactions release Si into porewaters, the saturation concentration of silica may be reached, which will inhibit weathering reactions until the porewater is recharged, or secondary silicate minerals precipitate (Köhler et al., 2010). Silica saturation, therefore, has the potential to slow enhanced weathering reactions and lower the CDR potential of EW. To assess this limitation (Köhler et al., 2010), modelled the outcomes of applying $1.58 \times 10^4$ Mt of olivine (~27 t $ha^{-1}$) onto the Amazon catchment and showed that silica saturation would reduce the carbon sequestration potential from 16 to 1.8 $GtCO_2$ $yr^{-1}$. The difference between these two values demonstrates the importance of understanding the role of silicic acid release and secondary mineral formation during enhanced weathering.

In this study, we address these two limitations to EW by combining observed river water geochemistry for major UK basins, with geochemical modelling and carbonate precipitation beaker experiments. Across 36 UK river catchments, we calculate how the application of EW to arable land will modify river alkalinity, pH, calcite saturation and thus the quantity of secondary carbonate formation. Along with investigating the possible decrease in CDR potential due to fluvial carbonate precipitation and silica saturation, this study also explores whether the shift in catchment chemistry caused by EW will be within boundaries acceptable for aquatic life.

## 2. Predicting the impact of carbonate precipitation and silica saturation on EW $CO_2$ sequestration

We calculate the potential reduction in EW efficiency due to carbonate and silica saturation, from a theoretical maximum, due to the

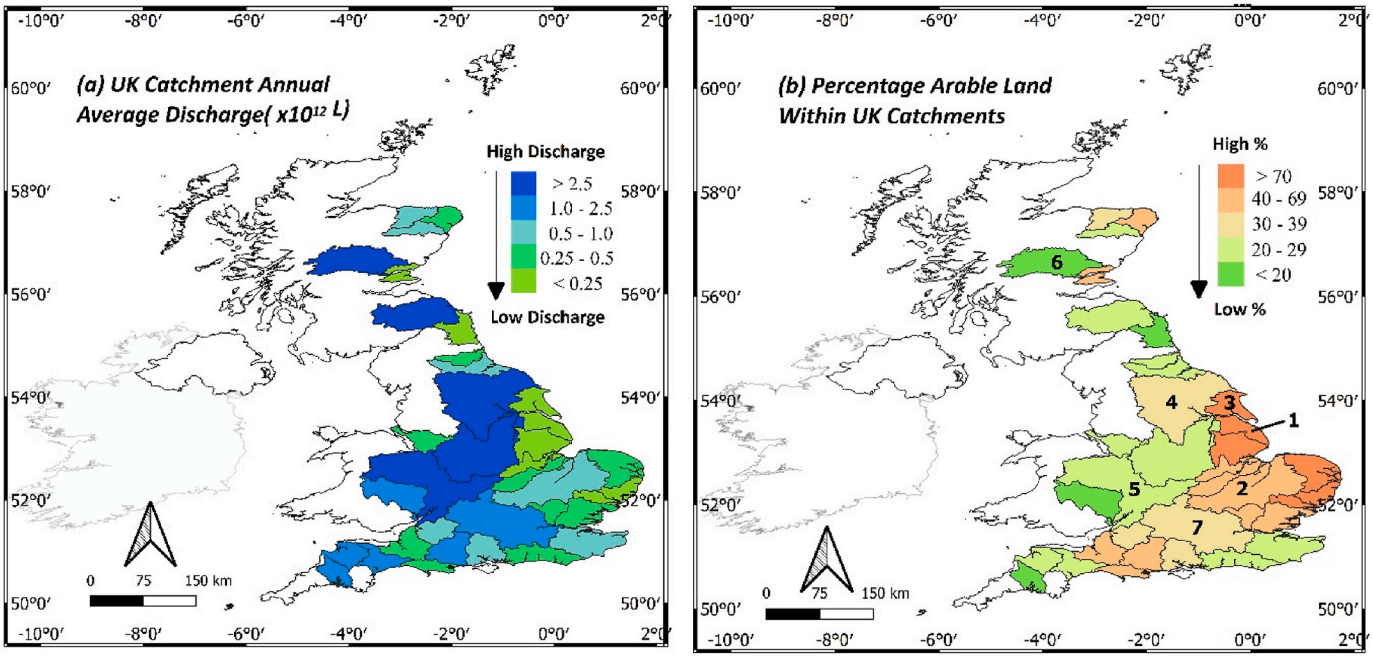


**Fig. 1.** (a) Average annual discharge per catchment studied ($10^{12}$ L $yr^{-1}$). (b) Percentage of arable land within each catchment. >90% of all UK arable land is located within the 36 catchments shaded in figures (a) and (b). Numbered catchments in (b) will be compared in detail within the results and discussion, chosen due to their differences in arable land%, discharge and bedrock lithology. (1 = Ancholme, 2 = Great Ouse, 3 = Hull, 4 = Ouse, 5 = Severn, 6 = Tay, 7 = Thames).

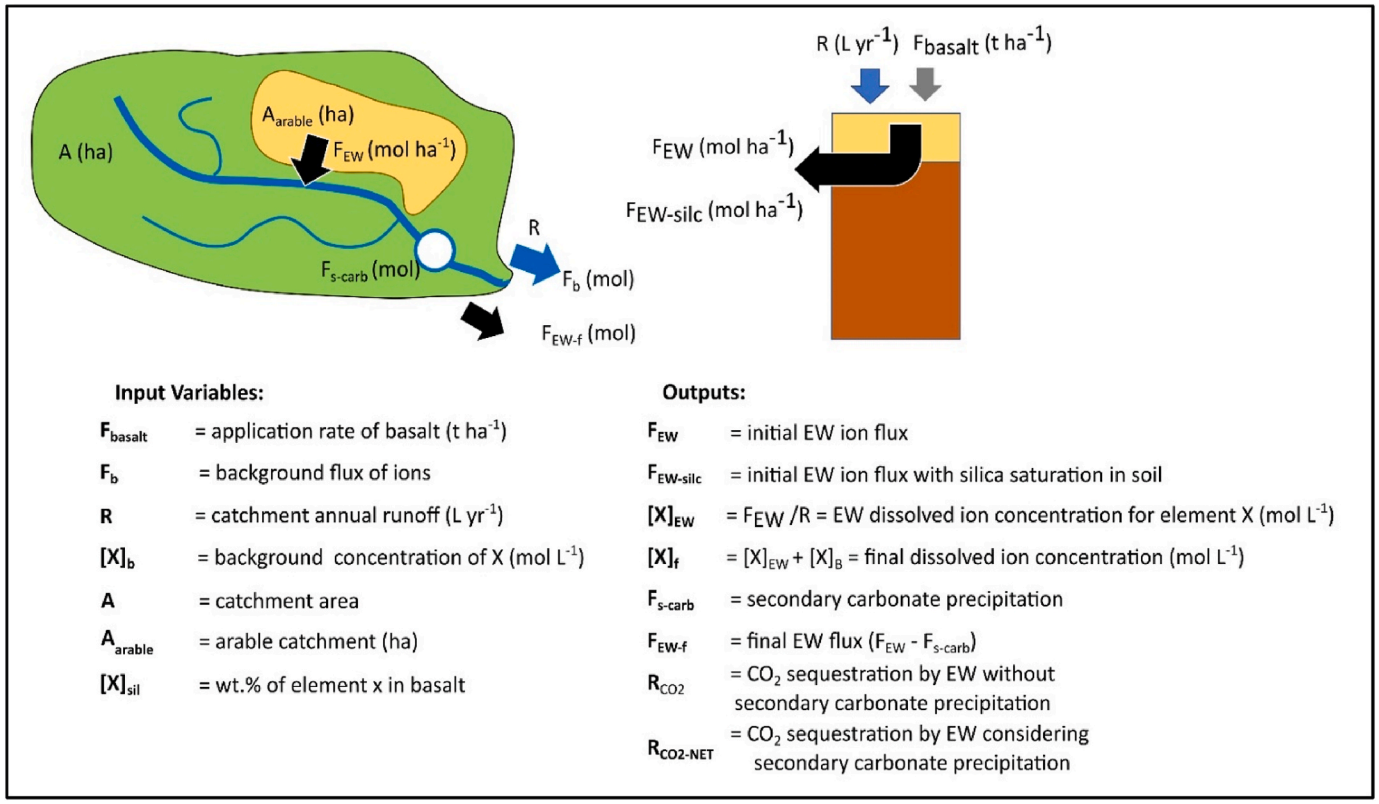


**Fig. 2.** A summary of the variables and terms used in the study. Input variables are obtained from natural catchment data, as discussed in the main text. Outputs are the variables derived in this study: $F_{EW}$ and $F_{EW-silc}$ are terms describing the flux of ions released from the applied basalt, which will be dependent on limitations by silica saturation ($F_{EW-silc}$) or carbonate saturation ($F_{EW-f}$) as discussed in section 3. $R_{CO2}$ is the maximum $CO_2$ drawdown expected from EW, and $R_{CO2-net}$ is the $CO_2$ drawdown once carbonate precipitation and silicic acid saturation are considered (section 5, and 7 respectively.

application of 10, 20 and 50 t $ha^{-1}$ of a compositionally average basalt (table 3, supplementary information) onto half of the arable land within major UK catchments (these values enable ready comparison with (Renforth 2012)). Basalt was used as the applied silicate, as it is likely to be the rock of choice for large-scale adoption of EW.

Catchment data is used to calculate the total amount of basalt applied per catchment. A total of ~5 Mha (Mha) of land is used for arable agriculture in the UK (The Royal Society and Royal Academy of Engineering, 2018), separated into ~90 catchments. Here we focus on 36 catchments which encompass 91% of this arable land (Fig. 1b). These are a subset of UK catchments with the highest percentage of arable land; it is considered that the remaining omitted catchments would contribute less to the total CDR of EW in the UK as they have minimal land available for the application of crushed silicates. Each catchment's total area $(A)$ was determined using the computer program qGIS and catchment boundaries from the Centre of Ecology and Hydrology (CEH, 2014), while the percentage of land that is arable ($A_{arable}$ -Fig. 2) is obtained from the National River Flow Archive (NRFA, 2023) (Fig. 1B, supplementary information-table 1).

We consider two possible scenarios of alkalinity release to the river, depending on the extent of EW silicate mineral dissolution (see section 3). These scenarios aim to explore the range in alkalinity release possible due to EW and reflect the uncertainty regarding the extent of a key inhibiting factor to dissolution: the degree that Si is released into porewaters. For each of these scenarios, we took the following steps to derive a reduced $CO_2$ sequestration budget.

i. Calculate the resulting riverine major ion chemistry and conservative alkalinity by combining baseline values with that released from EW in each catchment (section 3).
ii. Predict how the riverine pH is impacted by this increased alkalinity (section 6).
iii. Derive a threshold calcite saturation index at which rivers are expected to precipitate carbonate (section 4).
iv. Using the calculated ion chemistry, alkalinity, pH, the threshold saturation index for precipitation, and the geochemical model PHREEQC (version 3) (Parkhurst and Appelo, 2013), predict the change in calcite saturation index for each UK river and the amount of carbonate precipitation (section 5).
v. Use the percentage of ions which precipitate to calculate the reduced $CO_2$ sequestration due to carbonate precipitation and/or silica saturation (Section 5 and 7, respectively)

River geochemical data needed for step 1 was compiled from two UK Environmental Agency datasets (DEFRA, 2013, 2022) to determine the natural background flux of ions in each river ($F_B$; *Figure* 2,; supplementary information-table 2) and annual runoff information was obtained from the NRFA ($R$; Fig. 1a; Supplementary Information-table 1).

For simplicity, we have neglected the flux of ions to groundwater sources. According to research from UK Research and Innovation (UKRI), the annual recharge to UK aquifers is 7 billion $m^3\ yr^{-1}$ ($7 \times 10^{12}$ L $yr^{-1}$) (Bloomfield et al., 2013). Comparing this value to the UK annual riverine discharge to the ocean ($1.59 \times 10^{14}$ L $yr^{-1}$, calculated from the National River Flow Archive (NRFA) (Marsh et al., 2015), the average flux to groundwater is approximately 4.2% of the total UK water discharge. Therefore, we assume that the dissolved ion flux to groundwater will not significantly impact our calculations here.

## 3. Scenarios for alkalinity release from applied basalt to fluvial systems

The alkalinity released to rivers due to EW will depend on the basalt dissolution rate once applied to the field. Dissolution is limited by three main factors: (1) the supply of rock to the catchment, (2) kinetic factors limiting weathering, such as temperature, pH, presence of microbes, flux of water onto the catchment, and amount of available acid, and (3) equilibrium reactions in the soil porewaters. For the first factor, we consider three spreading scenarios: 10, 20 and 50 t $ha^{-1}$. For the second, we assume that the kinetic limitations have been minimised by increasing the reactive surface area by crushing the rock to ~10 μm (Hangx and Spiers, 2009) and applying the crushed basalt onto agricultural soils with low pH and high microbial activity that promote fast dissolution reactions (Renforth 2012; Beerling et al., 2018). In this section, we then consider the third factor: the impact of equilibrium reactions between the dissolving basalt and the accumulation of silicic acid products.

The fate of Si during basalt dissolution is unclear. Either dissolved silica will accumulate in porewaters which will eventually reach saturation, preventing further dissolution of the applied rock (Köhler et al., 2010). Alternatively, Si may be removed into Si bearing secondary minerals fast enough to prevent pore waters from reaching silica saturation (Schuiling et al., 2011). We model two end-member scenarios that capture this range of potential response to silicic acid saturation on the alkalinity released from basalt: $F_{EW}$, the maximum EW derived flux of ions to the river with no imposed limitation by silica saturation or kinetics (i.e. assuming all cations are released from complete basalt dissolution); and $F_{EW-silc}$, the flux caused by stringent silica saturation limitations in which water flux constrains the release of cations.

### 3.1. Scenario one: The maximum alkalinity released to rivers due to EW ($F_{EW}$)

The central assumption in this scenario is that basalt dissolution is not affected by silica saturation in soil pore waters. This may be due to (i) Si concentrations reducing through plant uptake (Cornelis et al., 2010) and/or incorporation into secondary Si bearing minerals which do not contain the four major mobile cations (Mg, K, Ca, Na), or (ii) by major cations being released from the rock faster than silica (Peters et al., 2004; Renforth et al., 2015). In both situations, major ions leave the site of weathering before silica saturation in soil porewaters is attained. In this scenario, we assume that the supply of rock to the cropland is the only limitation to basalt weathering (10–50 t $ha^{-1}$), and therefore, once the system reaches steady state, that all applied basalt dissolves within one year of application. Further, we assume that mobile cations $Ca^{2+}, Mg^{2+}, Na^{+}, K^{+}$ supplied in one annual addition are released over an annual timescale from the soil; that is, all cations in applied basalt are released as alkalinity into the catchment river (or rivers).

Other assumptions made when deriving $F_{EW}$ for this scenario:

i. *Al* and *Fe* from basalt dissolution are retained in soils (Renforth et al., 2015; Shao et al., 2016).
ii. $PO_4^{3-}$ (which makes up ~0.35 wt% of common basalts (Henderson and Henderson, 2009)) will remain in the soil profile absorbed onto secondary clays (Kantzas et al., 2022), or will be taken up by arable crops (Beerling et al., 2018).
iii. Other anions (e.g $Cl^{-}, NO_3^{-}, SO_4^{2-}$) are not significant in basalt composition (Supplementary information, table 3), and therefore remain at baseline values in rivers.

The ions contributing to the flux of EW alkalinity to the river $(F_{EW})$ for this scenario are the major cations (Ca, Mg, Na and K). Using catchment characteristics and the composition of basalt, the increased concentration of these ions ($[X]_f -$ Fig. 2) is calculated from their baseline concentration values $[X]_B$ (where X = Ca, Mg, K, Na) in each of the 36 catchments (supplementary information). The increased alkalinity from EW was then calculated by considering the charge balance in the river:

$$Conservative\ alkalinity = \sum charge\ of\ conservative\ cations\ \left(Ca^{2+}, Mg^{2+}, Na^{+}, K^{+}\right) - \sum charge\ of\ conservative\ anions\ \left(Cl^{-}, NO_3^{-}, SO_4^{2-}, PO_4^{3-}\right) \quad (4)$$

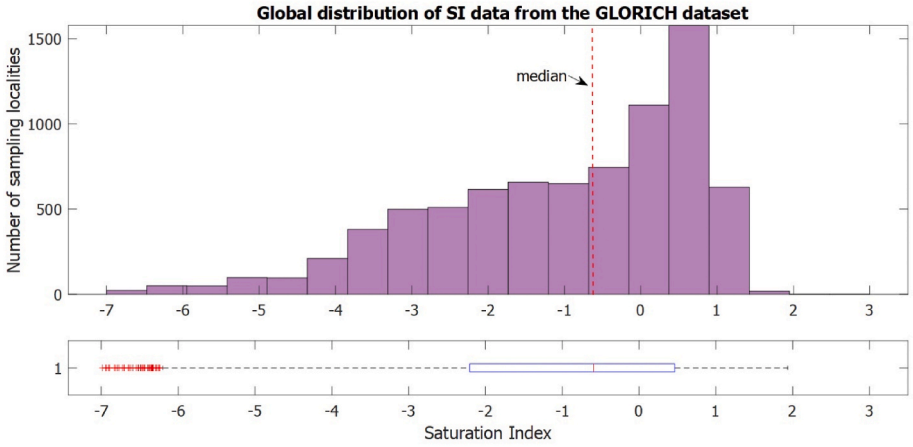


**Fig. 3.** Global river saturation index data obtained from the GLORICH database. Bottom plot represents the interquartile range of the global river calcite saturation indexes (median = −0.59, 25 percentile = −2.21, 75 percentile = 0.47) Database: Hartmann, J., Lauerwald, R. & Moosdorf, N. GLORICH- Global river chemistry database. PANGAEA (2019). doi:https://doi.org/10.1594/PANGAEA.902360.

The increase in cation flux to the water column is assumed to be balanced by an increase in carbonate species ($HCO_3^-$ and $CO_3^{2-}$). The alkalinity calculated for this scenario ($F_{EW}$) represents the maximum increase in each catchment due to EW. This scenario is therefore useful in constraining the maximum extent of secondary carbonate precipitation in UK rivers due to EW. However, we highlight that this is a theoretical maximum, and that while we assume that kinetic limitations could be minimised by a sufficiently small grain size and low pH conditions, some studies suggest that the dissolution of 10 μm basalt may take more than 10 years (Kelemen et al., 2020). Unfavourable weathering conditions, i.e. low water supply (Buckingham et al., 2022), may also slow the kinetics of weathering. Slow dissolution will of course lower the rate of alkalinity flux to the river calculated here.

### 3.2. Scenario two: The reduced EW alkalinity released to rivers due to limitations by silica saturation ($F_{EW-silc}$)

This scenario assumes that dissolution of minerals supplied by EW is limited by a saturation of Si in porewaters and provides a conservative estimate of EW effectiveness. In this scenario.

i. 100% of the weathered Si is released into porewater solution
ii. Silica saturation is reached when silicic acid concentration in soil porewater reaches 1.4 mmol $L^{-1}$, based on silica solubility equations (Henley 1983; Van Cappellen and Qiu, 1997) (included in supplementary information, and at 10 °C and at pH = 6)
iii. The amount of alkalinity transported from a catchment to a river is limited by the annual catchment runoff, which controls the recharge rate of porewaters (Köhler et al., 2010)
iv. Once saturation is reached, all remaining basalt is left undissolved on the catchment
v. *Fe* remains in the soil profile as Fe-oxides, or, in instances where *Fe* reaches the river, would mostly form iron hydroxides (at pH 7–8, the average pH of rivers), which are relatively insoluble (Neubauer et al., 2013).
vi. *Si* and *Al* are included in $F_{EW-silc}$ and, on entering the river system, are speciated according to the natural baseline riverine pH. Speciation was predicted using PHREEQC (version 3) (Parkhurst and Appelo, 2013) and was included in alkalinity equations.

Therefore, the major ions which contribute to the alkalinity flux in this scenario ($F_{EW-silc}$) are the major cations (Ca, Mg, Na, K), with an addition of Si and Al. The alkalinity flux $F_{EW-silc}$ derived from this scenario is useful in constraining the reduced flux under stringent silica limitations.

## 4. Determining the saturation state required for carbonate precipitation ($SI_{threshold}$)

Rivers may hold more EW alkalinity products in the dissolved load if they become supersaturated with respect to calcite (Knapp and Tipper, 2022). Predicting the quantity of secondary carbonate precipitation due to EW-derived alkalinity ($F_{s-carb}$) requires selection of a threshold saturation index at which rivers will precipitate carbonate ($SI_{threshold}$).

$SI_{Calcite}$ is defined by equation (5), e.g (Zeebe and Wolf-Gladrow, 2001):

$$SI_{Calcite} = log\left(\gamma Ca^{2+} * \gamma CO_3^{2-} / Ksp\right) \quad (5)$$

Where $\gamma Ca^{2+} * \gamma CO_3^{2-}$ are the activities of $Ca^{2+}$ and $CO_3^{2-}$ respectively, and *Ksp* is the equilibrium constant, which is dependent on salinity and temperature and is defined by (Mucci, 1983). In an ideal solution, when $SI_{Calcite} \geq 0$, it is saturated with respect to calcite, and secondary carbonate precipitation is expected (Zeebe and Wolf-Gladrow, 2001). In natural rivers, the $SI_{threshold}$ is often higher than $SI_{Calcite} = 0$, due to the inhibition of secondary mineral growth by the presence of specific ions in solution, such as $Mg^{2+}$, $SO_4^{2-}$, iron, phosphates, and organic molecules (Katz et al., 1993; Nielsen et al., 2016).

We estimate a $SI_{threshold}$ by considering the $SI_{Calcite}$ of natural rivers (section 4.1). To test the chosen $SI_{threshold}$ predicts accurate quantities of precipitation; simple beaker experiments were performed with UK river waters to compare with modelled precipitation values (section 4.2).

### 4.1. $SI_{Calcite}$ of global rivers

The global natural riverine distribution of $SI_{Calcite}$ in rivers can be examined using the global database GLORICH (Hartmann et al., 2019). This analysis suggests that ~39% of rivers are saturated or oversaturated with respect to calcium carbonate ($SI_{Calcite} > 0$) and 95% of the data have $SI_{Calcite} < 1$ (Fig. 3) All the UK rivers studied here also have median natural saturation indexes below 1 (ranging between −2.11 and + 0.86). Based on the scarcity of natural rivers with an $SI_{threshold} > 1$, a threshold saturation index of 1.0 was used in this study.

To confirm that carbonates will precipitate in rivers at this threshold value, we then explored locations where secondary carbonates form in rivers. Carbonate deposits are found along the Slovenian karstic River Krka (Zavadlav et al., 2017) in regions where $SI_{Calcite} = 0.8 - 1$, but not in locations where $SI_{Calcite} = 0.4$. In the Yalong river and tributaries (Chen et al., 2022), 80–90% of dissolved Ca is removed due to precipitation in rivers with a $SI_{Calcite} \sim 1$. In saturated rivers ($SI_{Calcite} =$

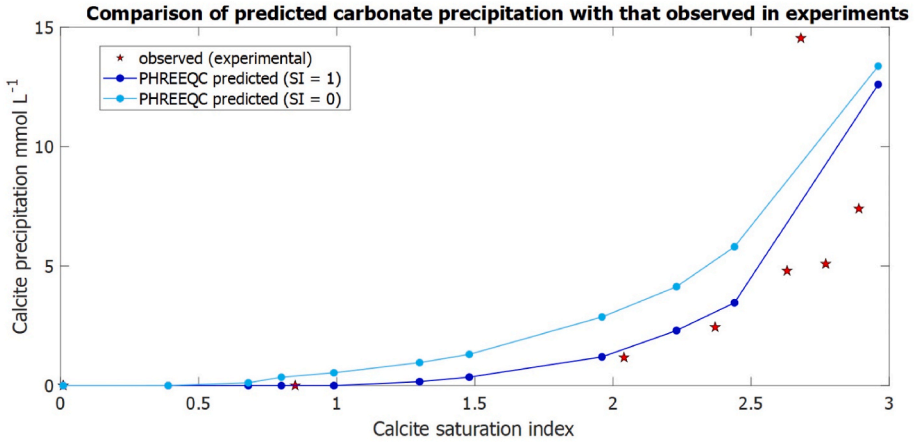


**Fig. 4.** Experimental confirmation that a threshold saturation index of 1.0 is realistic for carbonate precipitation in UK rivers. The figure compares the predicted amount of carbonate precipitation for a given saturation index, with those of the river water carbonate precipitation experiments of this study.

0.2–1.1) draining the Apennine Mountains (Italy), the fraction of Ca removed due to precipitation increases from 0.1 to 0.8 with increased $SI_{Calcite}$ (Erlanger et al., 2021). We also note that, independently to our analysis, a $SI_{Calcite} = 1.0$ was used in the study by (Knapp and Tipper, 2022) as the theoretical upper limit that rivers could reach prior to carbonate precipitation. Therefore, we expect that carbonate precipitation will occur in rivers with $SI_{Calcite} \geq 1.0$, and that using this as a baseline value in PHREEQC will provide conservative estimates for secondary precipitation in the UK rivers studied here.

### 4.2. River water carbonate precipitation experiments

River water carbonate precipitation experiments were carried out to provide an additional constraint on the saturation level required for carbonate precipitation in UK rivers and to test the selection of $SI_{threshold} = 1$. Unfiltered water from the River Thames and Severn was collected from accessible but flowing regions of both rivers (Supplementary Info-Fig. 1). The water was distributed into 500 ml beakers and alkalinity added which represented the two scenarios ($F_{EW}$ and $F_{EW-silc}$) for application rates 10, 20 and 50 t ha$^{-1}$. Changes to pH, alkalinity, the end dissolved chemistry, and the quantity and composition of the precipitate were measured to calculate the resultant $SI_{Calcite}$ and quantity of precipitation. The carbonate precipitation experiments were run for 4 days (Thames) and 5 days (Severn) to reflect the average time water will remain in each river (Worrall et al., 2014). A more detailed description of the experimental methodology is provided in the Supplementary Information.

Changes to the dissolved load over the course of the experiments suggest considerable carbonate precipitation. Dissolved $Ca^{2+}$ reduced in the beaker water column by 68.3% (10 t ha$^{-1}$), 94.7% (20 t ha$^{-1}$) and 99% (50 t ha$^{-1}$) in the Severn experiments, and by 92.2% (10 t ha$^{-1}$), 99.2% (20 t ha$^{-1}$) and 99.3% (50 t ha$^{-1}$) for the Thames, which has a naturally more saturated composition (supplementary information, table 7). In the beakers representing 20 and 50 t ha$^{-1}$, the final concentration of $Ca^{2+}$ was lower than in the control beaker. This implies carbonate precipitation in these beakers scavenged some of the natural $Ca^{2+}$ as well as the added $Ca^{2+}$. Concentrations of $Mg^{2+}$, $Na^{+}$ and $K^{+}$ remain elevated in the beakers for the duration of the experiment, indicating limited removal through secondary precipitation.

The starting $SI_{Calcite}$ of each beaker was determined using PHREEQC. To confirm the validity of using $SI_{threshold} = 1$, for any given initial $SI_{Calcite}$, the amount of precipitation in the beakers was compared to the amount predicted in PHREEQC using $SI_{threshold} = 1$ and $SI_{threshold} = 0$ and the predicted calculated riverine chemical changes due to 10–50 t ha$^{-1}$ application rates (section 5). Using $SI_{threshold} = 0$ tends to over-predict the quantity of carbonate, while $SI_{threshold} = 1$ aligns closer to the observed data (Fig. 4). Experiments confirm that using $SI_{threshold} = 1$ in PHREEQC will predict values of carbonate precipitation which may align closer to actual river values than those using $SI_{Calcite} = 0$.

The experiments were also useful to constrain the kinetics of secondary carbonate precipitation. Significant precipitation occurred within the timeframe of the experiment, suggesting that, if UK rivers are pushed over the $SI_{threshold}$ by EW, secondary carbonate precipitation will occur during river transport; before the products reach the ocean.

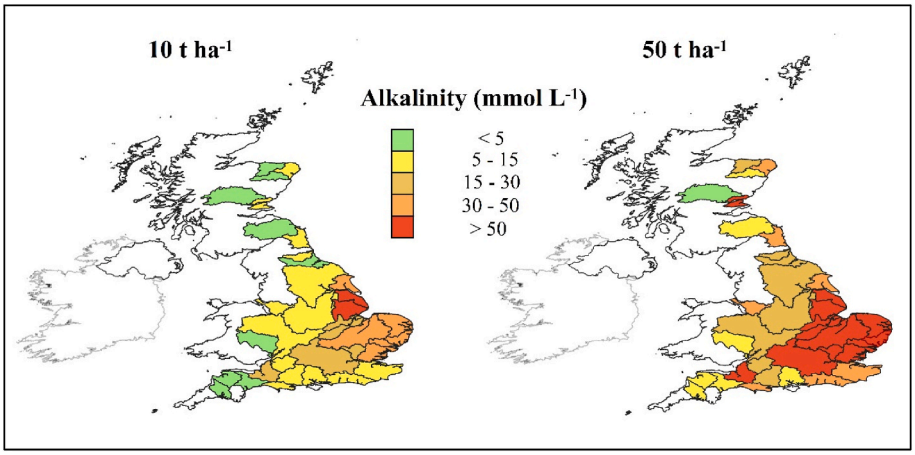


**Fig. 5.** Derived EW initial alkalinity changes in UK catchments due to spreading scenarios 10 and 50 t ha$^{-1}$ under scenario 1 in the absence of secondary carbonate precipitation and kinetic limitations. For comparison, the median natural alkalinity is 1.9 mmol L$^{-1}$. Alkalinity increase is calculated under the assumption that 10 and 50 t of basalt is applied to half of the available arable land in the catchment and that all the mobile cations Ca, Mg, Na and K within the basalt reach the river. River water flux used is the average discharge in each catchment (L yr$^{-1}$).

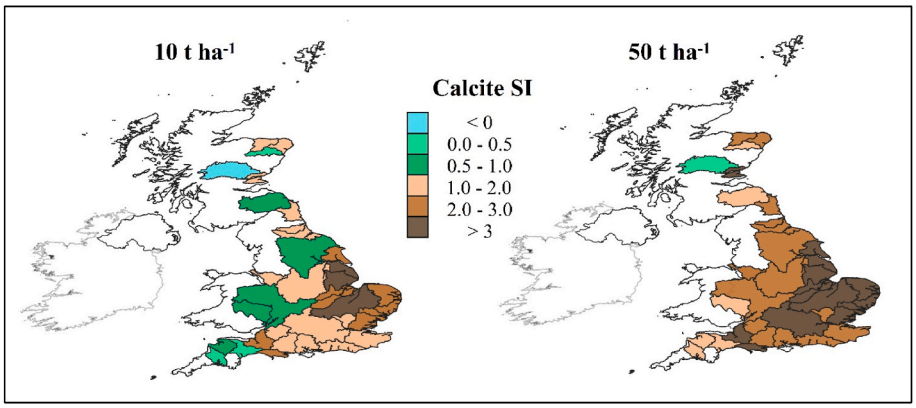


**Fig. 6.** Catchment calcite saturation indexes for the 10 t ha$^{-1}$ and the 50 t ha$^{-1}$ application rates under scenario 1 in the absence of calcite precipitation. Saturation Index values were obtained using PHREEQC, and the alkalinity and chemistry were calculated using assumptions discussed in (section 3). Brown colours on this figure represent catchments in which riverine carbonate precipitation is expected (i.e. SI > 1).

## 5. The impact of Scenario 1 (maximum alkalinity release) on UK river chemistry and the potential for $CO_2$ removal

Under scenario 1, where all basalt-derived alkalinity is released into rivers, the alkalinity flux resulting from application rates 10, 20 and 50 t ha$^{-1}$ ($F_{EW}$) would lead to significant increases in riverine alkalinity and therefore to carbonate precipitation (Figs. 5 and 8). For the 36 catchments in this study, and in the absence of carbonate precipitation, $F_{EW}$ would increase the river alkalinity to a maximum of 9.4 mmol/L$^{-1}$, 15.4 mmol L$^{-1}$ and 35.6 mmol L$^{-1}$ for 10, 20 and 50 t ha$^{-1}$, respectively. This is significantly higher than the natural value observed in UK rivers (median = 1.9 mmol L$^{-1}$). The extent of this increase is catchment specific and primarily reflects the ratio of arable land content to water flux; the Hull and the Great Ouse catchments, for example, would see large increases in alkalinity due to their extensive arable land (71% and 65% respectively) and relatively low discharge (Fig. 5).

In the absence of carbonate precipitation, the $SI_{Calcite}$ in many UK rivers will be pushed over the threshold needed for carbonate precipitation ($SI_{threshold} = 1$). The rivers studied here have natural calcite saturation indexes ranging between −2.11 and 0.86 (median = 0.125). Due to EW scenario 1, the median $SI_{Calcite}$ without carbonate precipitation increases to 1.75 (10 t ha$^{-1}$), 2.18 (20 t ha$^{-1}$) and 2.83 (50 t ha$^{-1}$), driving 26, 31 and 35 rivers over the $SI_{threshold}$.

To compare our results with (Zhang et al., 2022), we estimate the basalt application rate needed to achieve the $CO_2$ transport potential for global rivers as suggested in their study (i.e. 10 -12 Gt $CO_2$ for a $SI_{threshold} = 1$). For a basalt of average composition (Supporting Information, table 3), a maximum of 0.295 tonnes of $CO_2$ is removed for every tonne of basalt dissolved (i.e. see discussion, re: equation (7) below). 10–12 Gt $CO_2$ therefore corresponds to approximately 33.9–40.7 Gt basalt, which, if spread evenly over all global cropland (1.67 G Ha$^{-1}$, (FAO, 2020)), would equate to application rates of 24–29 t ha$^{-1}$ yr$^{-1}$. In other words (Zhang et al., 2022), show that rivers could hold the dissolved products of the complete dissolution of basalt applied at approximately 24–29 t ha$^{-1}$ yr$^{-1}$ before the threshold saturation index for precipitation is achieved.

However, we suggest that these limits would only be achieved in practise if the world's arable land was spread in such a manner that EW derived ions evenly distributed themselves into global rivers. The distribution of arable land in the UK is uneven, and therefore our results suggest that, for spreading scenarios of 10–50 t ha$^{-1}$, the impact on UK rivers $SI_{Calcite}$ is highly dependent on the quantity of arable land in the catchment (Fig. 1b. Fig. 6).

As scenario 1 would drive many UK rivers into disequilibrium with respect to calcite, PHREEQC predictions suggest that carbonate precipitation ($F_{s-carb}$) will occur to maintain river $SI_{Calcite} \leq 1$. We compared the quantity of Ca (and Mg) lost to carbonate precipitation predicted by PHREEQC with the initial EW derived alkalinity flux to the river (Fig. 5); the median amount of alkalinity lost to $F_{s-carb}$ in the 36 catchments studied was 6.2%, 10.4% and 31% for the 10, 20 and 50 t ha$^{-1}$ application rates respectively. Most of the reduction in alkalinity was from $Ca^{2+}$, which decreased in the dissolved load by an average of 18%, 38% and 82% for the 10, 20 and 50 t ha$^{-1}$ application rates (supplementary information-Fig. 2); however, some catchments also lost smaller amounts of $Mg^{2+}$ to Mg-rich carbonates.

The quantity of $CO_2$ consumed due to the complete dissolution of one tonne of basalt ($R_{CO_2}$) will be lowered by secondary carbonate precipitation (i.e., equations (1) and (2)). This reduction can be quantified by combining equations (6)–(8). $E_{pot}$ calculates the $CO_2$ consumed (in tonnes) by the percentage of EW derived alkalinity which remains dissolved until reaching the ocean, while $C_{pot}$ calculates the quantity of $CO_2$ consumed due to alkalinity lost by the formation of riverine secondary carbonates, after (Renforth, 2012, 2019):

$$R_{CO_2} = E_{pot} + C_{pot} \tag{6}$$

$$E_{pot} = M_{CO_2}/100 * \left( \%CaO/M_{CaO} + \%MgO/M_{MgO} + \%Na_2O/M_{Na_2O} + \%K_2O/M_{K_2O} \right) * w_1 \tag{7}$$

$$C_{pot} = M_{CO_2}/100 * \left( \%CaO/M_{CaO} + \%MgO/M_{MgO} \right) * w_2 \tag{8}$$

$M_{CaO}, M_{MgO}, M_{CO_2}, M_{Na_2O}$ *and* $M_{K_2O}$ are the molar mass of CaO, MgO, $CO_2$, $Na_2O$, and $K_2O$ respectively. $w$ refers to the molar amount of $CO_2$ that will be removed from the atmosphere for every mole of oxide dissolved from the rock. In Equation (7), the term $w_1$ is a correction to account for the carbon speciation in solution. It is 2 in pure water and decreases with increasing alkalinity to values as low as 1.4–1.7 in the ocean (Renforth and Henderson, 2017). On the basis that river waters flow to the sea, and to allow comparison with a previous study[5] we use $w = 1.7$. However, to highlight how the choice of $w$ would impact our results, we also calculate $E_{pot}$ using $w = 1.4$. Additional research to better constrain the $w$ factor would be valuable for future CDR budgets.

The $w$ value is impacted by the precipitation of carbonates: for calculation of $C_{pot}$, we used $w_2 = 1.0$ which is reduced from 1.7 due to the re-release of $CO_2$ during riverine precipitation (e.g., equation (2)). The presence of $CO_3^{2-}$ in solution will lower this value to <1, but we assume here that in fresh water, carbonate speciation is dominated by $HCO_3^-$ and therefore this reduction is assumed to be minimal.

The calculated $R_{CO_2}$ may also be reduced by the presence of $SO_3$ in the rock, which may lead to the release of $CO_2$ by the formation of acids,

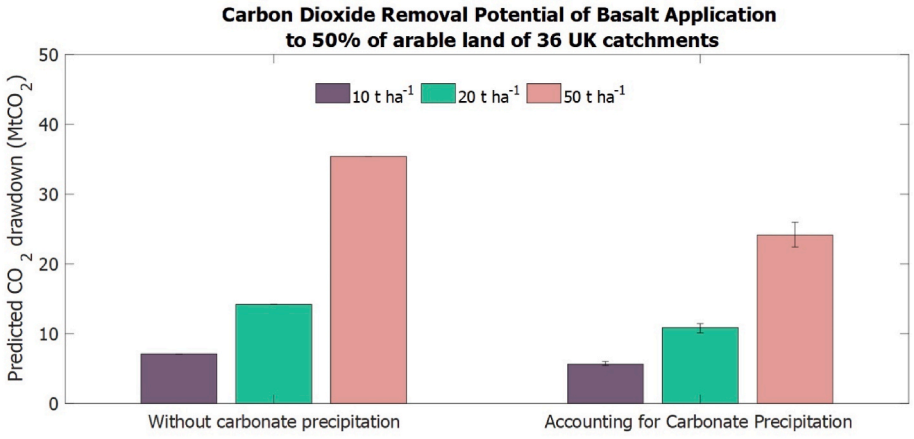


**Fig. 7.** Total $CO_2$ drawdown due to EW. (a) Without carbonate precipitation = the total quantity of $CO_2$ which could be sequestered due to the application of basalt onto 50% of the arable land of 36 UK catchments. (b) The revised quantity which includes secondary carbonate precipitation in the calculations. Both (a) and (b) are without secondary limitations on weathering by silicic acid saturation.

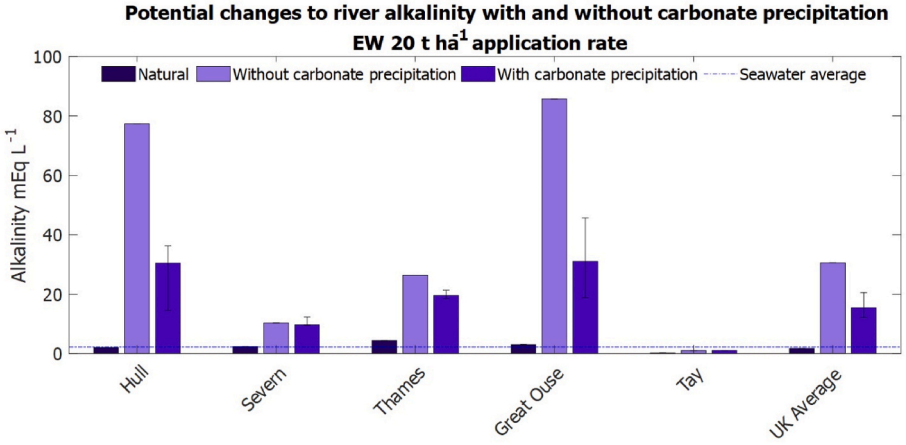


**Fig. 8.** Maximum alkalinity increase in 5 example UK rivers, with and without secondary carbonate precipitation, due to the dissolution of 20 t $ha^{-1}$ over half of the available land in the catchment. Values represent scenario 1 whereby all cations released reach the rivers. Alkalinity is compared to present-day average natural seawater levels (dashed line). Error bars represent the predicted amounts of carbonate precipitation, depending on the initial $pCO_2$ (see section 6).

as discussed in (Renforth, 2019), but here we assume a minimal contribution of $SO_3$ given typical basalt compositions (Supplementary Information, table 3), and on assumption basalt is most likely to be used for enhanced weathering.

The total annual $CO_2$ sequestration potential from EW for the 36 catchments was reduced due to carbonate precipitation (Fig. 7). The maximum sequestered $CO_2$ due to the application of 10, 20 and 50 t $ha^{-1}$ of basalt ($R_{CO2}$) across all 36 catchments is 8.3, 16.7 and 41.7 $MtCO_2$ respectively. However, with carbonate precipitation this reduces to 7.0 (+0.2, −0.4), 13 (+0.5, −0.9), and 30 (+1.2, −2.2) $MtCO_2$ for 10, 20 and t $ha^{-1}$ respectively (Fig. 7). Using $w_1 = 1.4$ in equation (7) (instead of $w_1 = 1.7$) , reduces these results to 6, 11 and 27 Mt $CO_2$ for 10, 20 and 50 t $ha^{-1}$ respectively.

Secondary carbonate precipitation during river transport of EW products is therefore expected to re-release 16% (+5%, −2%), 21% (+5%, −3%), and 27% (+5%, −3%) of the sequestered $CO_2$ from EW dissolution rates of 10, 20, and 50 t $ha^{-1}$ $yr^{-1}$ respectively. This calculated reduction in CDR due to carbonate precipitation (Fig. 7) assumes that the rivers in this study can maintain a supersaturation of $SI_{Calcite} = 1$. If UK rivers were to precipitate carbonates at a lower saturation index, (i.e. $SI_{Calcite} = 0 - 1$), then the result would be larger reductions to the EW CDR than that calculated here.

The CDR values expressed here represent conditions whereby rapid weathering occurs with little to no kinetic limitations. In the real soil conditions of the UK, some kinetic suppression of weathering would likely occur, the degree to which is currently debated. In (Kantzas et al., 2022) kinetic limitations were included in their model based study of EW in the UK, which suggested that the CDR potential of EW would reach 6–30 $MtCO_2$ $yr^{-1}$, after 30 years of repeated 40 t $ha^{-1}$ applications of 10–100 μm basalt particles. However, a significantly lower estimate (1.3 $MtCO_2$ $yr^{-1}$) was also derived from the results of a recent UK core study by (Buckingham et al., 2022). A one-off 100 t $ha^{-1}$ application of 125–250 μm basalt was mixed into the topsoil of a soil core from the southeast of England, and the subsequent slow basalt dissolution rates during the experimental period was attributed primarily to low water flux. The results of these two studies, and the subsequent discussion raised by (West et al., 2023 and Buckingham et al., 2023), highlights the importance of an accurate assessment of water flux when calculating/modelling EW dissolution rates and when upscaling CDR to regional or global levels.

The energy costs involved with mining, grinding, transportation and application will lower the net values for $CO_2$ sequestration predicted here. Moosdorf et al. (2012) suggest a 10–30% reduction in efficiency-primarily due to variations in energy needed to grind to different particle sizes (19.2%). Grinding to coarser sizes (greater than 10 μm) would lessen the energy requirements exponentially and reduce

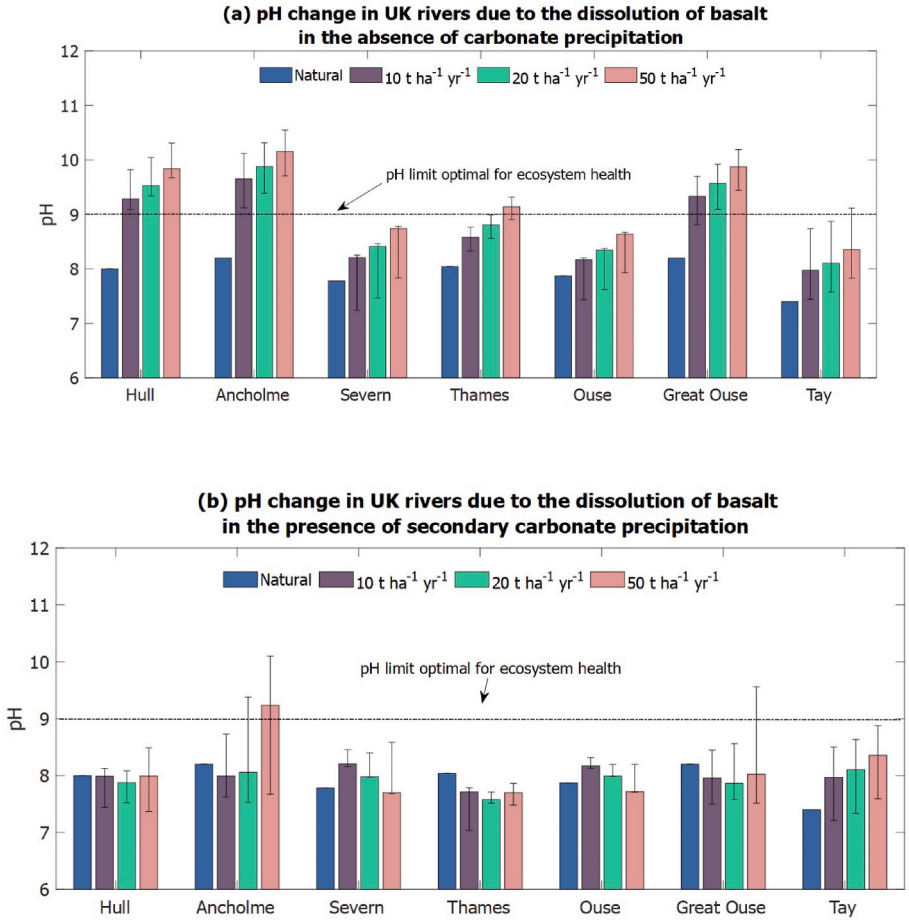


**Fig. 9.** Modelled pH change in 7 UK catchments as a function of basalt dissolution rate (10–50 t $ha^{-1}yr^{-1}$). (a) prior to carbonate precipitation, (b) post precipitation. Error bars are associated with the natural range in pCO2, upper bound = 95 percentile, lower bound = 5 percentile. Ecosystem pH limit line (pH > 9) based from values reported by the US Environmental Protection Agency (USEPA, 2022).

potential negative human respiratory impacts of fine dust, however this may come at a cost to $CO_2$ sequestration. The $CO_2$ release due to these processes may also be lowered by a switch to low carbon energy sources, i.e. solar, hydroelectric.

## 6. Impact on riverine pH

An increase in EW derived alkalinity to rivers will cause shifts in pH. We calculate this increase in riverine pH with and without carbonate precipitation. To do so we use conservative alkalinity, modified by addition of EW alkalinity, and the median natural riverine $pCO_2$ in the carbonate system equations (Zeebe and Wolf-Gladrow, 2001). Because the natural concentration of river $pCO_2$ varies by up to 2 orders of magnitude during the year (e.g. Supplementary Information, table 4), lower and upper $pCO_2$ bounds (5 and 95 percentile respectively) for each river were also used to provide an uncertainty range.

In the absence of carbonate precipitation, the addition of EW products from the complete dissolution of the applied silicate to rivers would result in large increases in pH (Fig. 9a). However, if carbonate precipitation removes excess alkalinity as expected, in most rivers pH will remain close to natural levels (Fig. 9b). These results indicate that secondary carbonate formation in rivers would be essential to buffer the potential pH increase caused by EW alkalinity addition and maintain riverine conditions suitable for freshwater ecosystems.

## 7. The impact of Scenario 2 (limitations caused by silica saturation) on UK river chemistry and EW CDR

The experiments and calculations in the previous sections have assumed that all major cations (Ca, Mg, Na and K) are fully released to rivers during EW basalt dissolution, without any limitation due to silica saturation (scenario 1). In scenario 2, where silica limitations are placed on weathering reactions, our calculations suggest that the release of cations ($F_{EW-silc}$) will be significantly reduced: leading to an increase in median river alkalinity only approximately double the natural median (from 1.9 to 3.6 mmol $L^{-1}$).

The lower degree of alkalinity released to rivers in scenario 2 prevents the degree of carbonate disequilibrium seen in scenario 1 (section 5). Nineteen rivers will remain under the $SI_{threshold}$ for carbonate precipitation, and the remaining rivers are driven between $SI_{Calcite} = 1.0 - 1.5$. Secondary carbonate precipitation presents only a marginal limitation to the riverine transport of EW products under scenario 2, removing between 0 and 7% of alkalinity from all rivers studied.

Under silica saturation, limited release of alkalinity to rivers, combined with the small secondary carbonate formation, reduces the CDR removal of EW in the 36 catchments to 0.23 $MtCO_2$ $yr^{-1}$. This large reduction in CDR due to silicic limitations may, in part, explain why there are some differences between CDR calculated from modelling studies and lab/field research.

We reviewed previous research to investigate the likelihood of silica saturation imposing such strict limitations suggested by the results of scenario 2. Results from (Peters et al., 2004; Renforth et al., 2015; Montserrat et al., 2017) suggest that during silicate weathering Si is

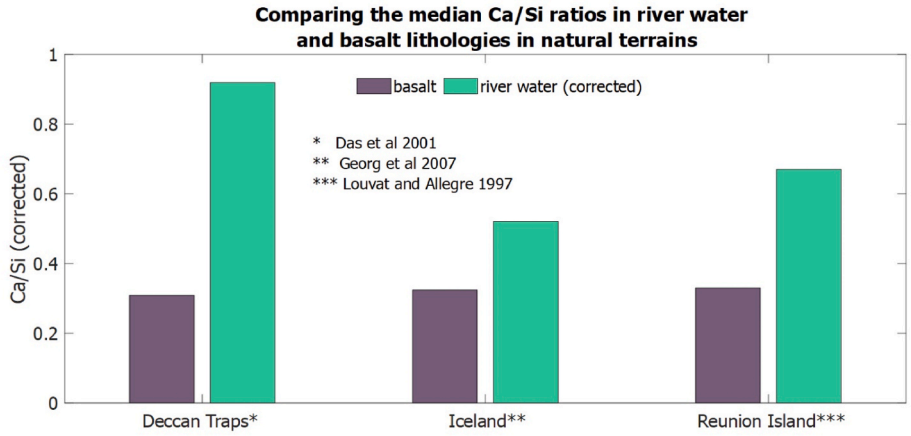


**Fig. 10.** Ca/Si ratio of basalt vs Ca/Si of the river water that flowed over it. Basalt composition from Reunion Island was taken from Fretzdorff and Haase, 2002), other basalt compositions came from Das et al., 2005) (Deccan Traps) and Georg et al., (2007) (Iceland). The concentration of Ca was corrected for other sources of Ca (carbonate, cyclic, evaporites), so that the Ca/Si corrected represented the Ca/Si in the water which came from basalt.

either-removed from solution via secondary Si bearing mineral formation, enriched within surface altered layers which have already preferentially released cations, or released into solution at a slower rate than cations. If Si is removed from solution faster than it accumulates, saturation may not be reached in porewaters. However, to get around the limitation of silica saturation, Si will need to remain in the soil in some form: either absorbed, within a cation impoverished surface layer in the added silicate or in a secondary mineral. This would drive significant change in soil properties, which would be compounded by the application of further silicates in future years and must be considered before the pursuit and upscaling of EW.

Some silica will likely be removed from the soil through plant uptake. Of the main crops known to accumulate Si, wheat, rice and sugarcane have the potential to remove the most bioavailable silica: up to 113, 470 and 700 kg $ha^{-1}$ $yr^{-1}$ respectively (Keeping 2017; Schaller et al., 2021). Annual harvesting removes the silica from the system along with the plant, depleting the soils of Si. It has therefore been suggested that the addition of silicate minerals for enhanced weathering could provide a secondary benefit for arable crops by replenishing this lost silica (Kelland et al., 2020; Manning 2022). Plants could help alleviate some of the silica saturation developed from EW dissolution reactions however, given the maximum values of Si uptake (between 0.113 and 0.7 t $ha^{-1}$, species dependent) and the typical application rates discussed in literature, significant quantities of Si would likely remain in the soil profile, either undissolved, or as silicic acid.

Preliminary evidence from natural weathering terrains suggests that twice as much Si is typically retained in soils as is transported to rivers during silicate weathering. This evidence is derived from the difference between $Ca*/Si_{river}$ (where * = corrected for other sources of dissolved $Ca^{2+}$, such as carbonates and rain) and the bedrock $Ca/Si_{basalt}$ in basaltic regions of Reunion Islands (Louvat and Allègre, 1997; Fretzdorff and Haase, 2002), the Deccan Traps (Dessert et al., 2001; Das et al., 2005), and Iceland (Georg et al., 2007). The rivers in all three regions are approximately twice as enriched in $Ca^{2+}$ than in Si, compared to the primary silicate rock (Fig. 10). Based on the riverine $Ca^{2+}$ enrichment under these weathering conditions, two times as much alkalinity is expected to be released during basalt weathering than that with stringent silica limitations. If conditions within the UK lead to similar weathering processes, then this would mean that the CDR potential calculated for realistic silica limitation would be approximately doubled (0.46 $MtCO_2$ $yr^{-1}$), but still suggests that silica saturation imparts a considerable limitation on EW.

## 8. Conclusions

This study presents an assessment of the limits on UK enhanced weathering due to the riverine transport of the chemical products. Calculations and experiments indicate that the complete dissolution of finely powdered basalt onto UK arable cropland will lead to significant shifts in river chemistry, resulting in substantial secondary carbonate precipitation. In the absence of silica saturation, riverine carbonate precipitation will reduce the CDR potential of EW by 16%, 21%, and 27% for application of 10, 20 and 50 t $ha^{-1}$ respectively.

Under rapid weathering conditions where all the applied basalt is dissolved, riverine secondary carbonate precipitation will be necessary to negate ecosystem damage from significantly higher pH values in river waters. In a theoretical upper limit whereby all dissolved rock reaches the river and without carbonate precipitation, many UK rivers would pH reach pH > 9. However, the secondary carbonate which is expected to precipitate will buffer much of this pH increase and bring most of the rivers studied here back to environmentally safe pH levels.

Silica saturation may place an additional limitation on EW. Placing strict silica saturation limitations on basalt dissolution significantly lowers the annual CDR potential of upscaling EW in the UK to a minimum of ~0.23 Mt $CO_2$ $yr^{-1}$, with consideration of the degree of silica saturation observed in other settings suggesting slight relaxation of this constraint and up to ≈0.5 Mt $CO_2$ $yr^{-1}$. In either case, Si saturation would lead to accumulation of Si-bearing minerals in soils and resulting shifts in soil properties which would need to be considered prior to the large-scale application of EW.

## Declaration of competing interest

The authors declare that they have no known competing financial interests or personal relationships that could have appeared to influence the work reported in this paper.

## Data availability

Data will be made available on request.

## Acknowledgements

The authors thank Phil Holdship and Katherine Clayton (University of Oxford) for assistance with data analysis (ICP-MS), and (XRD) respectively, as well as William Mayes, Don Porcelli, and David Hodkin for helpful discussions. Furthermore, we thank the editor and two anonymous reviewers who provided constructive comments that

enhanced the quality of the manuscript. This work was supported by the Natural Environment Research Council [Doctoral Training Program (DTP) RTSG code D4T00210 DG06.02].

## Appendix A. Supplementary data

Supplementary data to this article can be found online at https://doi.org/10.1016/j.apgeochem.2023.105643.

## References


Beerling, D.J., Kantzas, E.P., Lomas, M.R., Wade, P., Eufrasio, R.M., Renforth, P., et al., 2020. Potential for large-scale CO 2 removal via enhanced rock weathering with croplands. Nature 583 (July). https://doi.org/10.1038/s41586-020-2448-9.

Beerling, D.J., Leake, J.R., Long, S.P., Scholes, J.D., Ton, J., Nelson, P.N., et al., 2018. Farming with crops and rocks to address global climate, food and soil security. Nat. Plants 4 (6). https://doi.org/10.1038/s41477-018-0162-5, 392–392.

Bloomfield, J.P., Jackson, C.R., Stuart, M.E., 2013. *A Climate Change Report Card for Water Working Technical Paper 1 . Changes In Groundwater Levels , Temperature and Quality in the UK over the 20 Th Century : an Assessment of Evidence of Impacts from Climate Change* . 1–14. Retrieved from. http://nora.nerc.ac.uk/503271/).

Brantley, S.L., Shaughnessy, A., Lebedeva, M.I., Balashov, V.N., 2023. How temperature-dependent silicate weathering acts as Earth's geological thermostat. Science (New York, N.Y.) 379 (6630), 382–389. https://doi.org/10.1126/science.add2922.

Buckingham, F., Henderson, G.M., Holdship, P., Renforth, P., 2022a. Soil core study indicates limited CO2 removal by enhanced weathering in dry croplands in the UK. Appl. Geochem. 147 (October), 105482 https://doi.org/10.1016/j.apgeochem.2022.105482.

Buckingham, F., Henderson, G.M., Holdship, P., Renforth, P., 2023. Response to Comment from West et al. on "Soil core study indicates imited CO2 removal by enhanced weathering in dry croplands in the UK. Appl. Geochem. (in press).

CEH, 2014. Hydrometric Areas for Great Britian and Northern Ireland. NERC-Environmental Information Data Centre. https://doi.org/10.5285/1957166d-7523-44f4-b279-aa5314163237. (Accessed 1 July 2022).

Chen, B.B., Li, S.L., Pogge von Strandmann, P.A.E., Wilson, D.J., Zhong, J., Sun, J., Liu, C. Q., 2022. Calcium isotopes tracing secondary mineral formation in the high-relief Yalong River Basin, Southeast Tibetan Plateau. Sci. Total Environ. 827, 154315 https://doi.org/10.1016/j.scitotenv.2022.154315.

Cornelis, J.T., Delvaux, B., Cardinal, D., André, L., Ranger, J., Opfergelt, S., 2010. Tracing mechanisms controlling the release of dissolved silicon in forest soil solutions using Si isotopes and Ge/Si ratios. Geochem. Cosmochim. Acta 74 (14), 3913–3924. https://doi.org/10.1016/j.gca.2010.04.056.

Das, A.D., Krishnaswami, S., Sarin, M.M., Pande, K., 2005. Chemical Weathering in the Krishna Basin and Western Ghats of the Deccan Traps , India, vol. 69, pp. 2067–2084. https://doi.org/10.1016/j.gca.2004.10.014, 8.

DEFRA, 2013. Historic UK water quality sampling harmonised monitoring scheme detailed data. Available at: https://data.gov.uk/dataset/bda4e065-41e5-4b78-b405-41c1d3606225/historic-uk-water-quality-sampling-harmonised-monitoring-scheme-summary-data. (Accessed 4 December 2022).

DEFRA, 2022. Water Quality Archive. Retrieved August 1, 2022, Available at: https://www.nationalarchives.gov.uk/doc/open-government-licence/version/3/. (Accessed 1 June 2022).

Dessert, C., Dupré, B., François, L.M., Schott, J., Gaillardet, J., Chakrapani, G., Bajpai, S., 2001. Erosion of Deccan Traps determined by river geochemistry: impact on the global climate and the 87 Sr/86 Sr ratio of seawater. Earth Planet Sci. Lett. 188 (3–4), 459–474. https://doi.org/10.1016/S0012-821X(01)00317-X.

Erlanger, E.D., Rugenstein, J.K.C., Bufe, A., Picotti, V., Willett, S.D., 2021. Controls on physical and chemical denudation in a mixed carbonate-siliciclastic orogen. J. Geophys. Res.: Earth Surf. 126 (8), 1–24. https://doi.org/10.1029/2021JF006064.

FAO, 2020. Land use in agriculture by numbers. Available at: https://www.fao.org/sustainability/news/detail/en/c/1274219/. (Accessed 12 March 2023).

Fretzdorff, S., Haase, K.M., 2002. Geochemistry and petrology of lavas from the submarine flanks of Réunion Island (western Indian Ocean): implications for magma genesis and the mantle source. Mineral. Petrol. 75 (3–4), 153–184. https://doi.org/10.1007/s007100200022.

Fuhr, M., Geilert, S., Schmidt, M., Liebetrau, V., Christoph, V., Ledwig, B., Wallmann, K., 2021. Kinetics of olivine weathering in seawater: an experimental study. Front. Clim. 4 (March), 1–20. https://doi.org/10.7185/gold2021.7375.

Georg, R.B., Reynolds, B.C., West, A.J., Burton, K.W., Halliday, A.N., 2007. Silicon Isotope Variations Accompanying Basalt Weathering in Iceland, vol. 261, pp. 476–490. https://doi.org/10.1016/j.epsl.2007.07.004.

Hangx, S.J.T., Spiers, C.J., 2009. International Journal of Greenhouse Gas Control Coast. Spread. Olivine Control Atmospher. CO 2 Concentrat. : A critical analysis of viability 3, 757–767. https://doi.org/10.1016/j.ijggc.2009.07.001.

Hartmann, J., Lauerwald, R., Moosdorf, N., 2019. GLORICH- Global River Chemistry Database. https://doi.org/10.1594/PANGAEA.902360.

Hartmann, J., West, J., Renforth, P., Köhler, P., La De Rocha, C.L., Wolf-Gladrow, D.A., et al., 2013. Enhanced chemical weathering as a geoengineering strategy to reduce atmospheric carbon dioxide, a nutrient source and to mitigate ocean acidification: (accepted article). Philoso. Transact. Royal Soc. (2012) 113–150. https://doi.org/10.1002/rog.20004.

Henderson, P., Henderson, G.M., 2009. The Cambridge Handbook of Earth Science Data. Cambridge University Press, UK.

Henley, R.W., 1983. pH and silica scaling control in geothermal field development. Geothermics 12 (4), 307–321. https://doi.org/10.1016/0375-6505(83)90004-4.

IPCC, 2018. Summary for policymakers. In: Masson-Delmotte, V., Zhai, P., Pörtner, H.-O., Roberts, D., Skea, J., Shukla, P.R., Pirani, A., Moufouma-Okia, W., Péan, C., Pidcock, R., Connors, S., Matthews, J.B.R., Chen, Y., Zhou, X., Gomis, M.I., Lonnoy, E., Maycock, T., Tignor, M., Waterfield, T. (Eds.), Global Warming of 1.5°C. An IPCC Special Report on the Impacts of Global Warming of 1.5°C above Pre-industrial Levels and Related Global Greenhouse Gas Emission Pathways, in the Context of Strengthening the Global Response to.the Threat of Climate Change, Sustainable Development, and Efforts to Eradicate Poverty.

Kantzas, E.P., Val Martin, M., Lomas, M.R., Eufrasio, R.M., Renforth, P., Lewis, A.L., et al., 2022. Substantial carbon drawdown potential from enhanced rock weathering in the United Kingdom. Nat. Geosci. 15 (5), 382–389. https://doi.org/10.1038/s41561-022-00925-2.

Katz, J.L., Reick, M.R., Herzog, R.E., Parsiegla, K.I., 1993. Calcite growth inhibition by iron. Langmuir 9 (5), 1423–1430. https://doi.org/10.1021/la00029a043.

Keeping, M.G., 2017. Uptake of silicon by sugarcane from applied sources may not reflect plant-available soil silicon and total silicon content of sources. Front. Plant Sci. 8 (May), 1–14. https://doi.org/10.3389/fpls.2017.00760.

Kelemen, P.B., McQueen, N., Wilcox, J., Renforth, P., Dipple, G., Vankeuren, A.P., 2020. Engineered carbon mineralization in ultramafic rocks for CO2 removal from air: review and new insights. Chem. Geol. 550 (May), 119628 https://doi.org/10.1016/j.chemgeo.2020.119628.

Kelland, M.E., Wade, P.W., Lewis, A.L., Taylor, L.L., Sarkar, B., Andrews, M.G., et al., 2020. Increased yield and CO2 sequestration potential with the C4 cereal Sorghum bicolor cultivated in basaltic rock dust-amended agricultural soil. Global Change Biol. 26 (6), 3658–3676. https://doi.org/10.1111/gcb.15089.

Klemme, A., Rixen, T., Müller, M., Notholt, J., Warneke, T., 2022. Destabilization of carbon in tropical peatlands by enhanced weathering. Nat. Commun. 1–9. https://doi.org/10.1038/s43247-022-00544-0.

Knapp, W.J., Tipper, E.T., 2022. The efficacy of enhancing carbonate weathering for carbon dioxide sequestration. Front. Clim. https://doi.org/10.3389/fclim.2022.928215.

Köhler, P., Hartmann, J., Wolf-Gladrow, D.A., 2010. Geoengineering potential of artificially enhanced silicate weathering of olivine. Proc. Natl. Acad. Sci. U. S. A 107 (47), 20228–20233. https://doi.org/10.1073/pnas.1000545107.

Louvat, P., Allègre, C.J., 1997. Present denudation rates on the Island of Reunion determined by river geochemistry: basalt weathering and mass budget between chemical and mechanical erosions. Geochem. Cosmochim. Acta 61 (17).

Manning, D.A.C., 2022. Mineral stabilities in soils: how minerals can feed the world and mitigate climate change. Clay Miner. 1–10. https://doi.org/10.1180/clm.2022.17.

Marsh, T., Sanderson, F., Swain, O., 2015. Derivation of the UK National and Regional Runoff Series. Retrieved from. http://nora.nerc.ac.uk/id/eprint/510580.

Montserrat, F., Renforth, P., Hartmann, J., Leermakers, M., Knops, P., Meysman, F.J.R., 2017. Olivine dissolution in seawater: implications for CO2 sequestration through enhanced weathering in coastal environments. Environ. Sci. Technol. 51 (7), 3960–3972. https://doi.org/10.1021/acs.est.6b05942.

Moosdorf, N., Hartmann, J., Du, H.H., Meybeck, M., Kempe, S., Curie, M., et al., 2012. The Geochemical Composition of the Terrestrial Surface (without Soils) and Comparison with the Upper Continental Crust, pp. 365–376. https://doi.org/10.1007/s00531-010-0635-x.

Mucci, A., 1983. The solubility of calcite and aragonite in seawater at various salinities, temperatures, and one atmosphere total pressure. Am. J. Sci. 283, 780–799.

Neubauer, E., Köhler, S.J., Von Der Kammer, F., Laudon, H., Hofmann, T., 2013. Effect of pH and stream order on iron and arsenic speciation in boreal catchments. Environ. Sci. Technol. 47 (13), 7120–7128. https://doi.org/10.1021/es401193j.

Nielsen, M.R., Sand, K.K., Rodriguez-Blanco, J.D., Bovet, N., Generosi, J., Dalby, K.N., Stipp, S.L.S., 2016. Inhibition of calcite growth: combined effects of Mg2+ and SO42-. Cryst. Growth Des. 16 (11), 6199–6207. https://doi.org/10.1021/acs.cgd.6b00536.

NRFA, 2023. UK National River Flow archive. Available at: https://nrfa.ceh.ac.uk. (Accessed 1 January 2023).

Parkhurst, D., Appelo, C.A., 2013. Description of Input and Examples for PHREEQC Version 3—A Computer Program for Speciation, Batch-Reaction, One-Dimensional Transport, and Inverse Geochemical Calculations. U.S. Geological Survey Techniques and Methods. https://doi.org/10.3133/tm6A43.

Peters, S.C., Blum, J.D., Driscoll, C.T., Likens, G.E., 2004. Dissolution of wollastonite during the experimental manipulation of hubbard brook watershed. Biogeochemistry 67 (3), 309–329. https://doi.org/10.1023/B:BIOG.0000015787.44175.3f.

Pogge von Strandmann, P.A.E., Tooley, C., Mulders, J.J.P.A., Renforth, P., 2022. The dissolution of olivine added to soil at 4°C: implications for enhanced weathering in cold regions. Front. Clim. 4 (February), 1–11. https://doi.org/10.3389/fclim.2022.827698.

Renforth, P., 2012. The potential of enhanced weathering in the UK. Int. J. Greenh. Gas Control 10, 229–243. https://doi.org/10.1016/j.ijggc.2012.06.011.

Renforth, P., Henderson, G.M., 2017. Assessing ocean alkalinity for carbon sequestration. Rev. Geophys. 55 (3), 636–674. https://doi.org/10.1002/2016RG000533.

Renforth, P., Pogge von Strandmann, P.A.E., Henderson, G.M., 2015. The dissolution of olivine added to soil: implications for enhanced weathering. Appl. Geochem. 61, 109–118. https://doi.org/10.1016/j.apgeochem.2015.05.016.

Renforth, Phil, 2019. The negative emission potential of alkaline materials. Nat. Commun. 10 (1) https://doi.org/10.1038/s41467-019-09475-5.

Schaller, J., Puppe, D., Kaczorek, D., Ellerbrock, R., Sommer, M., 2021. Silicon cycling in soils revisited. Plants 10 (2), 1–36. https://doi.org/10.3390/plants10020295.

Schuiling, R.D., Wilson, S.A., Power, L.M., 2011. Enhanced silicate weathering is not limited by silicic acid saturation. Proc. Natl. Acad. Sci. U. S. A 108 (12), 2011. https://doi.org/10.1073/pnas.1019024108.

Shao, S., Driscoll, C.T., Johnson, C.E., Fahey, T.J., Battles, J.J., Blum, J.D., 2016. Long-term responses in soil solution and stream-water chemistry at Hubbard Brook after experimental addition of wollastonite. Environ. Chem. 13 (3), 528–540. https://doi.org/10.1071/EN15113.

The Royal Society and Royal Academy of Engineering, 2018. Greenhouse Gas Removal. Report by the UK Royal Society and Royal Academy of Engineering.

USEPA, 2022. US environmental protection agency. pH, in causal analysis/diagnosis decision information system (CADDIS). Avaliable at: https://www.epa.gov/caddis-vol2/caddis-volume-2-sources-stressors-responses-pH#-high. (Accessed 1 August 2022).

Van Cappellen, P., Qiu, L., 1997. Biogenic silica dissolution in sediments of the Southern Ocean. I. Solubility. Deep-Sea Res. Part II Top. Stud. Oceanogr. 44 (5), 1109–1128. https://doi.org/10.1016/S0967-0645(96)00113-0.

Vicca, S., Goll, D.S., Hagens, M., Hartmann, J., Janssens, I.A., Neubeck, A., et al., 2022. Is the climate change mitigation effect of enhanced silicate weathering governed by biological processes? Global Change Biol. 28 (3), 711–726. https://doi.org/10.1111/gcb.15993.

West, L.J., Banwart, S.A., Martin, M.V., Kantzas, E., Beerling, D.J., 2023. Making mistakes in estimating the CO2 sequestration potential of UK croplands with enhanced weathering. Appl. Geochem. 151, 105591 https://doi.org/10.1016/j.apgeochem.2023.105591.

Worrall, F., Howden, N.J.K., Burt, T.P., 2014. A method of estimating in-stream residence time of water in rivers. J. Hydrol. 512, 274–284. https://doi.org/10.1016/j.jhydrol.2014.02.050.

Zavadlav, S., Rožic, B., Dolenec, M., Lojen, S., 2017. Stable isotopic and elemental characteristics of recent tufa from a karstic Krka River (south-east Slovenia): useful environmental proxies? Sedimentology 64 (3), 808–831. https://doi.org/10.1111/sed.12328.

Zeebe, R.E., Wolf-Gladrow, D.A., 2001. CO2 in seawater: equilibrium, kinetics, isotopes. In: Elsevier Oceanography Series Book, Vol. 65).first ed. Elsevier.

Zhang, S., Planavsky, N.J., Katchinoff, J., Raymond, P.A., Kanzaki, Y., Reershemius, T., Reinhard, C.T., 2022. River chemistry constraints on the carbon capture potential of surficial enhanced rock weathering. Limnol. Oceanogr. 67 (S2) https://doi.org/10.1002/lno.12244.